

Article

Water-Stressed Plants Do Not Cool: Leaf Surface Temperature of Living Wall Plants under Drought Stress

Michael Gräf ^{1,*},[†] , Markus Immitzer ^{2,†} , Peter Hietz ³ and Rosemarie Stangl ^{1,*} 

¹ Institute of Soil Bioengineering and Landscape Construction, University of Natural Resources and Life Sciences, Vienna (BOKU), Peter-Jordan-Straße 82, 1190 Vienna, Austria

² Institute of Geomatics, University of Natural Resources and Life Sciences, Vienna (BOKU), Peter-Jordan-Straße 82, 1190 Vienna, Austria; markus.immitzer@boku.ac.at

³ Institute of Botany, University of Natural Resources and Life Sciences, Vienna (BOKU), Gregor-Mendel-Straße 33, 1180 Vienna, Austria; peter.hietz@boku.ac.at

* Correspondence: michael.graef@boku.ac.at (M.G.); rosemarie.stangl@boku.ac.at (R.S.)

† These authors contributed equally to this work.

Abstract: Urban green infrastructures offer thermal regulation to mitigate urban heat island effects. To gain a better understanding of the cooling ability of transpiring plants at the leaf level, we developed a method to measure the time series of thermal data with a miniaturized, uncalibrated thermal infrared camera. We examined the canopy temperature of four characteristic living wall plants (*Heuchera x cultorum*, *Bergenia cordifolia*, *Geranium sanguineum*, and *Brunnera macrophylla*) under increasing drought stress and compared them with a well-watered control group. The method proved suitable to evaluate differences in canopy temperature between the different treatments. Leaf temperatures of water-stressed plants were 6 to 8 °C higher than those well-watered, with differences among species. In order to cool through transpiration, vegetation in green infrastructures must be sufficiently supplied with water. Thermal cameras were found to be useful to monitor vertical greening because leaf surface temperature is closely related to drought stress. The usage of thermal cameras mounted on unmanned aerial vehicles could be a rapid and easy monitoring system to cover large façades.

Keywords: urban green infrastructure; plant water stress; uncalibrated thermal camera; cooling potential; urban heat island; monitoring



Citation: Gräf, M.; Immitzer, M.; Hietz, P.; Stangl, R. Water-Stressed Plants Do Not Cool: Leaf Surface Temperature of Living Wall Plants under Drought Stress. *Sustainability* **2021**, *13*, 3910. <https://doi.org/10.3390/su13073910>

Academic Editor: Venkat Sridhar

Received: 12 February 2021

Accepted: 30 March 2021

Published: 1 April 2021

Publisher's Note: MDPI stays neutral with regard to jurisdictional claims in published maps and institutional affiliations.



Copyright: © 2021 by the authors. Licensee MDPI, Basel, Switzerland. This article is an open access article distributed under the terms and conditions of the Creative Commons Attribution (CC BY) license (<https://creativecommons.org/licenses/by/4.0/>).

1. Introduction

In the 21st century, a major challenge for urban areas is to cope with the increasing ambient air temperature due to the urban heat imbalance [1]. This is largely caused by the increased absorption of shortwave radiation and the excessive release of anthropogenic heat, as well as the decreased latent heat transfer [2]. This has serious implications for the economic costs and social well-being in cities, such as a doubling of the energy consumption to cool buildings, an increase in peak electricity demand, and a significant increase in heat-related mortality during summer periods [3–5]. It has long been known that urban heat islands (UHIs) occur in densely built-up areas and can be 5–6 °C warmer than the surrounding landscape [6]. Therefore, adequate and sustainable urban planning that mitigates the consequences of global increases in temperatures and the associated negative effects on human health is necessary [7–10]. This includes the use of materials such as thermochromic or radiative cooling structures to decrease the urban temperature or the intensive use of urban greenery and water for evaporative cooling [11]. Among those technologies, green infrastructures (GIs) offer strategies to provide ecosystem services to mitigate the temperature increase in urban areas [12]. GI, such as building greenery, uses seminatural features that can modify urban warming through evaporative cooling, shading, and the modification of airflows [7,13,14]. By promoting thermal comfort, they

contribute to the health and well-being of urban residents, which has received increasing attention over the last two decades due to the worsening consequences of climate change and the rapidly increasing population in cities [15,16].

In densely built-up areas without space for parks or tree plantings, green roofs and façades are promising GIs for cooling [16]. Green roofs with drought-resistant vegetation, high water retention, and storage capacity do not require external irrigation [17]. Vertical green is categorized into living wall systems (LWSs), where plants directly grow on the wall rooting in a suspended substrate, and green façades, where plants root in ground-based soil [18,19]. While green façades mainly use climbing plants, the choice of plants in LWS is almost unlimited. Regardless of the GI used, whether a park, a tree, a green roof, or façade, the central elements are plants [7,20,21]. Shading and evapotranspiration contribute most to the cooling effect of the plants [22]. The denser the plant canopy, the higher the cooling potential, as long as plants are sufficiently supplied with water for transpiration [23]. The potential cooling effect of plants on air temperature is highest in the warmest periods of the year and hottest hours during the day when potential evapotranspiration is highest. However, it is severely reduced under conditions when soil water is limiting, which results in drought stress and lower transpiration because stomata close [7,24–26]. Therefore, GIs often rely on external irrigation, as precipitation is insufficient, especially under warm and dry conditions.

The energy balance of leaves, or any other bodies, depends on radiative, sensible, and latent energy exchange [27]. During the day, plants absorb more radiation (visible and infrared) than they emit. This net absorption of radiation is balanced by latent heat loss via transpiration and the convective transfer of heat to the air. The higher the transpiration, the less heat will be given off to the air. If more energy is lost via transpiration than gained by the radiation exchange, then leaves effectively cool the surrounding air by convective energy transfer from the air to maintain the energy balance [28]. If not absorbed by vegetation, radiation will be absorbed by surfaces that do not evaporate water, which drives the surface energy balance upwards [29]. Stomata close under drought stress, reducing evaporative cooling due to the lack of transpiration, and leaves warm-up [30]. Stomatal conductance (g_s) to water vapor estimates the physical resistance to the movement of gases between the air and the interior of the leaf and is closely related to the canopy temperature [31,32]. Plant-based approaches such as measuring stomatal conductivity or water potential are typically used to detect drought stress [28]. However, this is not practical for monitoring GI as it is too labor intensive, not suitable for automation, and, furthermore, façade greening is often not accessible for these measurements.

Infrared thermography is a noncontact alternative to monitor GI from a distance that can be used to measure the surface temperature, including that of leaves affected by evaporative cooling. The canopy temperature (T_C) is responsive to water stress and therefore can be used as an indicator for water stress levels in plants [33]. One way to determine the level of stress in plants is to compare the temperature of a well-watered crop canopy, with water-stressed plants at the same stage of growth. The difference between stressed and non-stressed plant canopy temperature is expressed as degrees above non-stressed (DANS) [34]. Early work measured accumulated T_C differences of stressed and non-stressed plant canopies with point measurements at a specific time per day [35]. The majority of water stress indices use T_C as a single daily measurement during the time of maximal stress or by evaluating the time above a temperature threshold [36]. This method is sensitive to small stresses and dependent on stomatal closure as an early indicator of water deficits [28]. However, little attention was given to the use of T_C over longer time-periods, so far. Especially for plants used in building greenery, such information is scarce, as the method has been applied mainly in crops. Evaluating the time threshold requires a continuous measurement of canopy and weather parameters, which demands more intensive sensing and data-logging instrumentation and maintenance [34]. Highly accurate thermal sensors use quantum detectors with short response times and very high sensitivities but require external cooling, which makes them bulky and expensive [37].

The initial objective of this study was to identify a simple method to determine the T_C over a longer period using a miniaturized, uncalibrated thermal infrared (TIR) camera. Such cameras are suitable for use with unmanned aerial vehicles (UAVs), but they are usually not radiometrically calibrated, so they only provide information on relative temperatures expressed in raw digital numbers (DNs) [38]. To obtain absolute values, a thermal calibration must be performed before each use. For our purpose, we used a Vue pro 640 (FLIR Systems Inc., Wilsonville, OR, USA) and took pictures every minute for the duration of the experiment and developed a method to evaluate the images. We investigated the temperature differences between stressed and non-stressed plants to gain a better understanding of the cooling potential of transpiring plants

The aim of our study was: (1) to develop a simple method using an uncalibrated TIR camera to continuously monitor plant canopy temperature; and (2) to assess the canopy temperature differences between well-watered and water-stressed plants, which are commonly used in LWS. While the cooling effect of GIs is usually evaluated using the ambient temperature as an indicator, we focused on plant leaves [39,40]. Therefore, we also measured stomatal conductance to directly quantify water stress in the plants.

2. Materials and Methods

Data for the study were collected in a greenhouse experiment by testing four different species commonly used in LWS. After an initial acclimatization of 21 days, half of the plants continued to be well-watered, while irrigation was stopped for the other half. We continuously recorded thermal data of the plant canopy until water-stressed plants had withered (leaves turned brown).

2.1. Experimental Design

On 8 April 2019, ten specimens each of *Brunnera macrophylla*, *Geranium sanguineum*, *Bergenia cordifolia*, and *Heuchera x cultorum* were precultivated in 11 × 11 cm pots with 1.0 L of substrate (Stender C200; Schermbeck, Germany) for 21 days in a greenhouse at the University of Natural Resources and Life Sciences, Vienna (Austria). During this period, we irrigated each pot twice a day (9 a.m. and 6 p.m.) with 150 mL in each irrigation run. To maintain 100% water holding capacity (WHC), pressure-compensated drip hoses with a flow rate of 4 L/h (Delta™ Drp Spike PC; Trani, Italy) were used. After acclimatization until 29 April 2019, we evenly divided the plants into water-stressed pots that were no longer irrigated and a control group kept at 100% WHC (Figure 1). With these irrigation settings, we monitored the plants until those under water stress had withered, which took between 18 and 27 days depending on the species.

2.2. Growing Conditions

We measured air temperature and relative humidity using an Atmos 14 sensor (Meter Group; Pullman, Washington, USA) and solar radiation flux density using a PYR total solar radiation sensor (Meter Group). A ZL6 data logger (Meter Group) connected all sensors with 10 min intervals. During the experiment, the average temperature in the greenhouse was 14.7 °C (5.4–32.5 °C), humidity was 62% (21%–89%), and solar radiation was 180 W/m² (0–1065 W/m²).

2.3. Thermal Data Recording

Thermal images of the plants were recorded every minute, starting on 25 April 2019 until 26 May 2019 with a Vue Pro 640 (FLIR Systems, Inc.; Wilsonville, Oregon, USA) at a distance of 1.5 m above the plants (Figure 1). Recordings were saved as 14-bit tiffs with a resolution of 640 × 512 pixels without postprocessing. We then created shapefiles with the software ArcGIS (Version 10.2 Esri; Redlands, CA, USA) containing polygons covering the five plants per species and treatment (Figure 2). Because the position of the plants changed slightly, mainly due to growth, the polygons were adjusted daily.

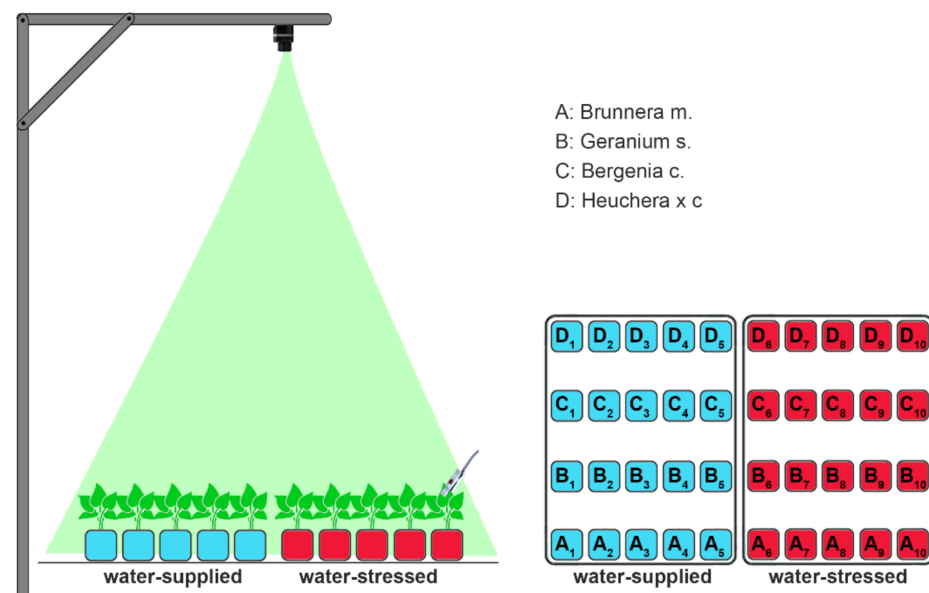


Figure 1. Schematic representation of the data acquisition of the thermal camera installed above the plants and the experimental setup: five individuals per species were cultivated in the respective irrigation setting. Red refers to the group with water stress and blue to the water-supplied group. The white clip characterizes the periodic porometer measurements.

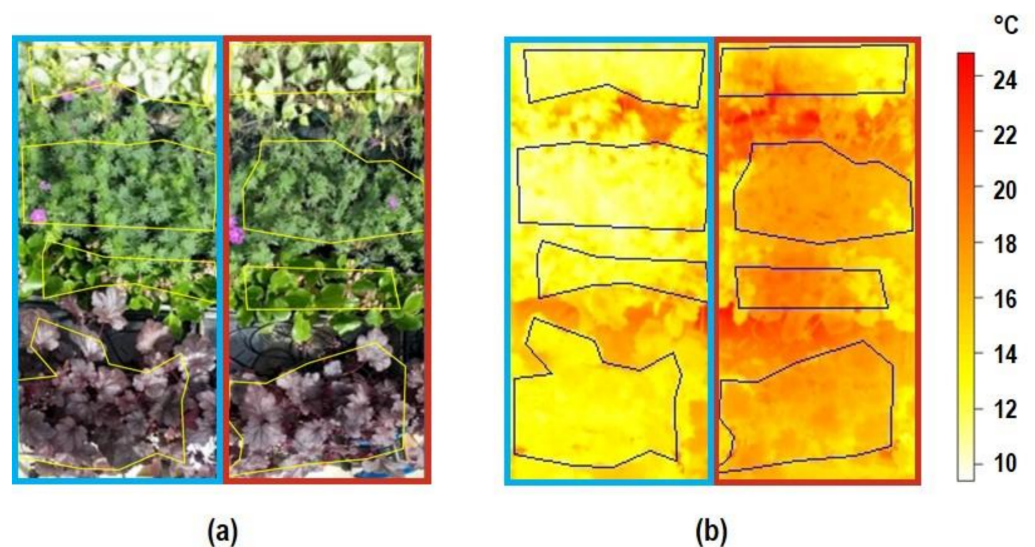


Figure 2. (a) RGB image of the plants in the experimental setup on 10 May 2019 at 14:00. (b) Thermal image at the same time, the polygons (yellow in (a), black in (b)) outline the groups of plants per species and treatment (red frame refers to the water stress and blue frame to the control group). Images were not recorded orthogonally referenced.

We extracted the radiometric values (DN) with the software RStudio (Version 1.1.463 R Studio, Boston, Massachusetts, USA) from each pixel within the polygons and calculated the median and the 97.5 percentile [41]. Because the differences between the treatments were clearer with the 97.5 percentile, we subsequently used these data. Extracted time series data then were smoothed using the Whittaker–Henderson approach with lambda 1600 and $d = 1$ using the R Studio package *pracma* [42,43]. For the transformation from raw digital numbers (DN) recorded by the thermal camera into degrees Celsius, we used the equation:

$$T [^{\circ}\text{C}] = \text{DN} \times 0.04 - 303.72 \quad (1)$$

following the linear model of Kelly [38] for an ambient air temperature of 10 °C. This model requires calibration for different temperatures, and the values for the plant canopy temperature therefore do not represent absolute temperature values [44]. We thus used the temperature differences (ΔT in °C) between the canopy temperatures of the stressed (T_S) and the nonstressed (T_{NS}) plants.

2.4. Stomatal Conductance

On Days 4, 9, 14, 17, 21, and 24 after the end of the acclimatization phase, leaf stomatal conductance was measured between 11:00 and 13:00 on one fully developed marked leaf of each plant (five plants per treatment, four species, two treatments), with a leaf porometer (AP-4, Delta-T Devices; Cambridge, UK). Time series of stomatal conductivity were analyzed with a two-way repeated-measures ANOVA using 5% as the level of significance with the *rstatix* package (Version 0.6.0) [45]. The normal distribution of the residuals was verified visually with Q-Q plots. Assumption of sphericity was controlled with Mauchly's test of sphericity. We performed a paired *t*-test to find differences between g_s and water treatments at the time of measurement using the Bonferroni correction.

3. Results

3.1. Canopy Temperature

Figure 3 shows T_S , T_{NS} , and ΔT , as well as air temperature and radiation, in *Brunnerna* before drought stress (27 to 30 April, Figure 3a,c) and 9 to 11 May after water was withheld from the stress treatment (Figure 3b,d). When all plants were equally irrigated, T_S and T_{NS} were nearly identical, with a mean and maximal ΔT of 0.2 and 0.7 °C, respectively. Leaf temperatures were lowest during hours of maximum air temperature and radiation.

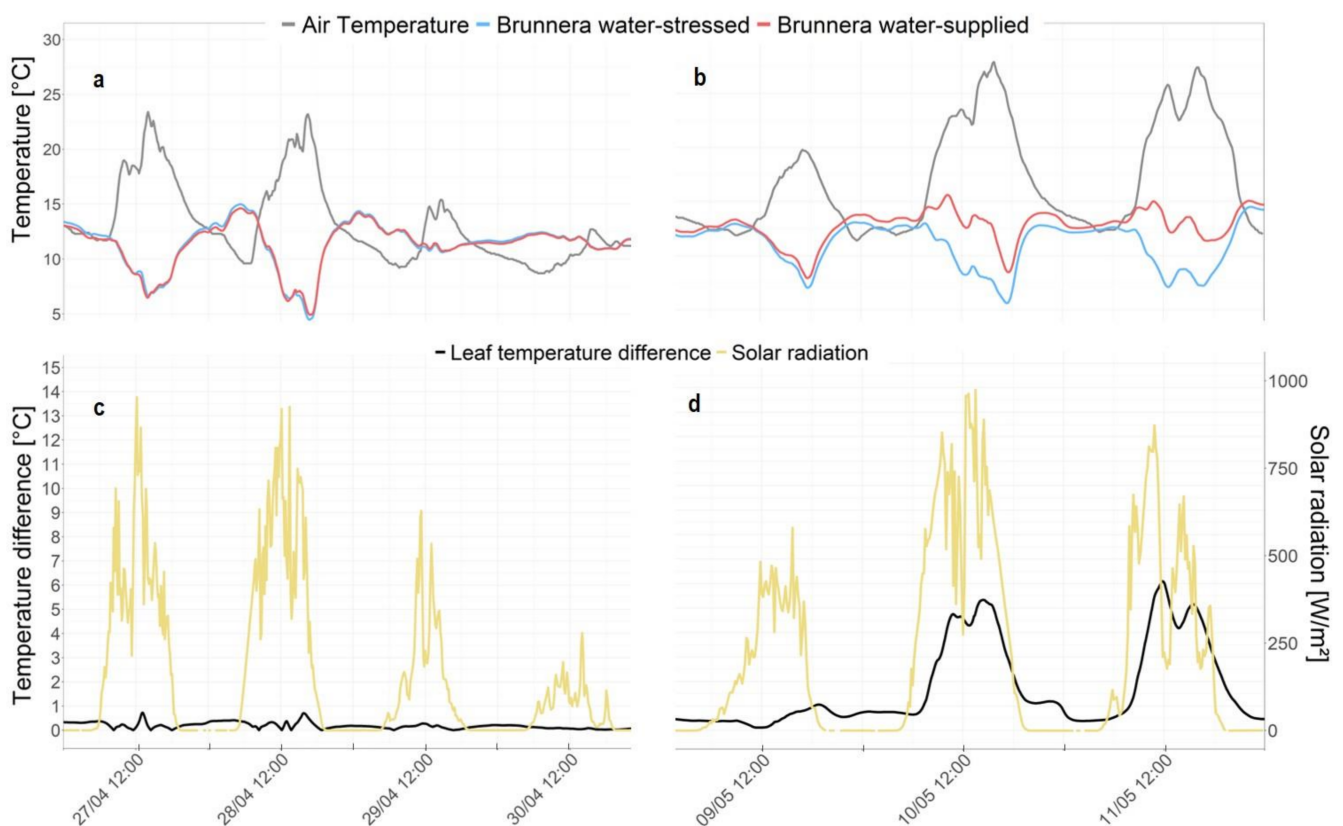


Figure 3. Leaf surface temperatures of the water-stressed (red) and irrigated (blue) plants of *Brunnerna macrophylla* during the acclimatization phase (a) and the transition into drought stress (b). Panels (c) and (d) show the difference in temperature ΔT between the stressed and nonstressed plants (continuous line) and solar radiation (dotted line).

Ten days after the last irrigation (9 May), the ΔT (Figure 3d) reached a maximum of 1°C . On this day, air temperature and radiation were low. During the subsequent days, the two curves diverged and the temperature differences rose to 5.4°C . Leaf temperatures during daylight were still slightly lower than during the night, and the maximum ΔT was around noon when air temperature and radiation were also highest. At night, the two curves converged again and the temperature differences did not exceed 1°C , even when one treatment was water-stressed.

Leaf surface temperatures of *Geranium*, *Bergenia*, and *Heuchera* followed a similar pattern. We selected three time windows, the first within the acclimatization phase from 27 April to 30 April, the second under moderate stress (9 May to 11 May), and the third with peak stress from 16 May to 19 May. The mean difference in leaf surface temperatures during the acclimatization period was 0.2°C for *Geranium*, 0.3°C for *Bergenia*, and 0.3°C for *Heuchera* between the two groups during the acclimatization phase (Figure 4). The maximal short-term temperature difference during this period was 1.6°C in *Heuchera*.

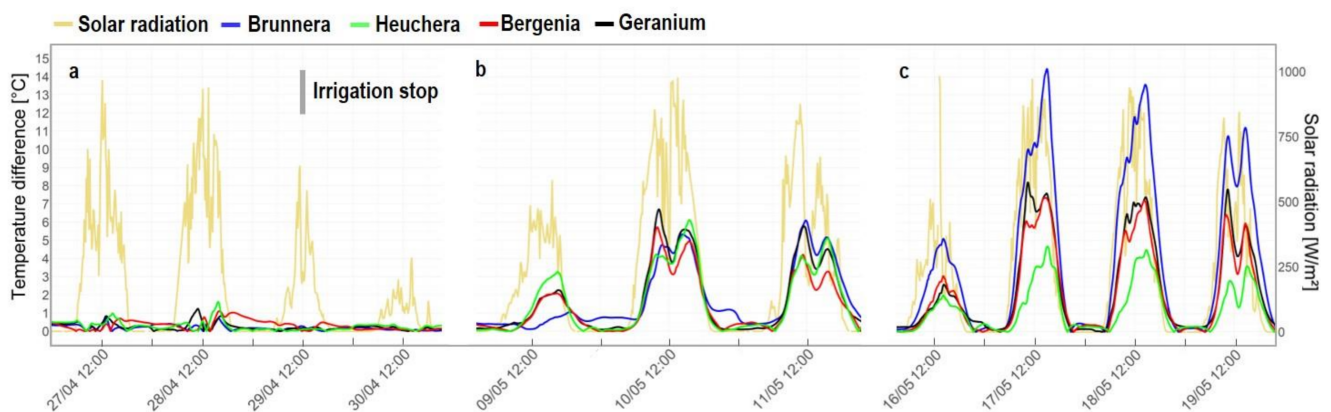


Figure 4. Temperature differences (ΔT) between water-stressed and well-watered plants during the experiment, at the beginning (a), in the middle (b), and toward the end (c) of the stress experiment.

Ten days after the last irrigation of the stress group (9 May), the maximum ΔT was 2.2°C in *Geranium*, 2.0°C in *Bergenia*, and 3.1°C in *Heuchera*. The next day, the temperature differences rose to 6.7 , 5.7 , and 6.5°C for *Geranium*, *Bergenia*, and *Heuchera*, respectively. At this point, the water stress started to become visible in the species *Brunnera*, which had individual wilting leaves. Among the other species, there was no stress indication observable, but temperatures of stressed leaves were clearly higher than in the control plants. On 13 May, 14 days after irrigation stopped, water stress symptoms were visible on all plants. After 18 days, the leaves of *Brunnera* were completely withered, at which time the images can no longer be used as T_C because the camera recorded mostly the soil in the pots. The highest ΔT before plants wilted were 6.1°C in *Brunnera*, 8.2°C in *Geranium*, 7.4°C in *Bergenia*, and 6.5°C in *Heuchera*, always around solar noon. During the night, water stress was not visible in the TIR, and T_{NS} and T_S hardly differed.

3.2. Stomatal Conductance

The two-way ANOVA revealed a significant interaction between treatment (water-stressed and control) and time. We, therefore, analyzed the effect of the treatment for each measurement day. On 3 May, five days after the last irrigation of the stress group, g_s of control and water-stressed *Brunnera* (276 vs. 221 $\text{mmol}/\text{m}^2/\text{s}$) and *Bergenia* (228 vs. 200 $\text{mmol}/\text{m}^2/\text{s}$) did not differ significantly (Figure 5). In *Geranium* (329 vs. 112 $\text{mmol}/\text{m}^2/\text{s}$) and *Heuchera* (199 vs. 66 $\text{mmol}/\text{m}^2/\text{s}$), g_s of drought-stressed plants were significantly lower than in control plants. Depending on the species, drought stress was visible early through stomatal conductance, this effect increases with time. Nine days after irrigation stopped (9 May), g_s was significantly lower in all stressed plants as stomata were respond-

ing to drought stress in all species. *Geranium* and *Heuchera* responded faster than *Brunnera* and *Bergenia*. The reduced transpiration as a consequence of lower g_s caused the leaf surface temperature to increase under the influence of solar radiation.

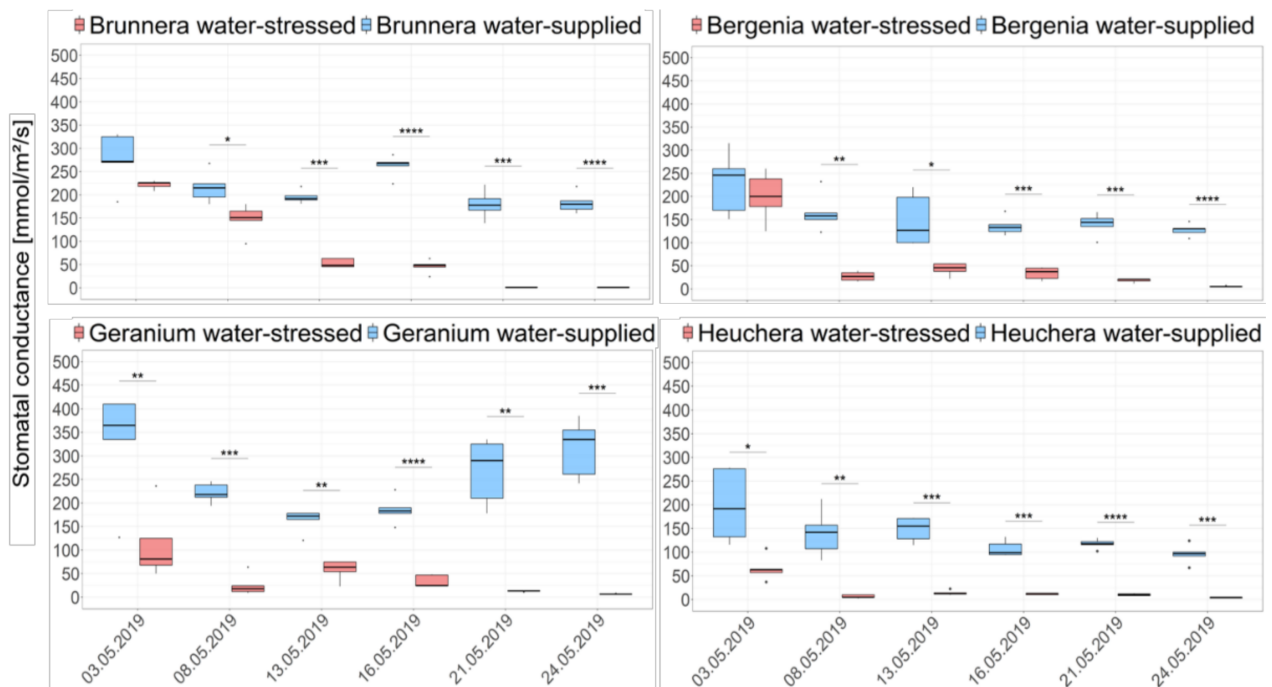


Figure 5. Development of the stomatal conductivity of the tested plant species measured 3, 5, 7, 9 and 12 days after drought stress imposition. Level of significance is indicated by star code * $p < 0.05$, ** $p < 0.01$, *** $p < 0.001$, and **** $p < 0.0001$.

4. Discussion

The initial objective of this study was to test a method to measure the leaf surface temperature over time using a miniaturized, uncalibrated TIR camera. This permits measuring whole-canopy temperature, which is preferable to point measurements of selected leaves where the variation in leaf angles influences the measurements [46]. To obtain absolute temperature values in a time series with a TIR camera, continuous reference measurements of a known object, typically a blackbody, and the sources of radiation are required [47]. However, absolute values are not always necessary, especially to monitor temperature trends over time, and we found that the calibration of the camera with a line equation was sufficient [37]. We studied temperature differences (ΔT) between water-stressed and well-watered plants, which proved satisfying and yielded novel data for urban GI research.

The most obvious finding was the identical leaf temperature of the stressed and non-stressed plants during and shortly after the acclimatization period, regardless of the species. ΔT were within a range of maximum 1 °C, with one deviation due to the species *Heuchera* of up to 1.6 °C. Figure 3 shows the transition from well-watered to water stress for the species *Brunnera* from Days 10 to 12, when the temperature difference increased from a maximum of 1.0 °C up to 6.1 °C, while, simultaneously, stomatal conductivity decreased. One of the first investigations of the canopy temperature with infrared thermometry was carried out by Tanner [48], who found a maximum temperature difference of 3 °C between stressed and non-stressed potato plants (*Solanum tuberosum*). Taghaeian et al. [34] recorded differences up to 7.0 °C in sunflower (*Helianthus annuus*). In contrast to the methods described above, which used point measurements, we analyzed the temperatures of the entire canopy and extracted the 97.5 percentile, which proved more practical for an applied setting to detect drought stress. In our study, the highest ΔT were 6.1 °C for *Brunnera*, 6.5 °C for *Heuchera*, 7.4 °C for *Bergenia*, and 8.2 °C for *Geranium*. Under hot and dry conditions,

ΔT between stressed and non-stressed canopies are greatest [49]. This was also evident in our results, where ΔT of all species followed the ambient temperature so that, on a colder day, differences were smaller than on a warmer day. Leaf temperature depends on climatic conditions such as radiation, air temperature, and wind speed, as well as canopy characteristics such as morphology, density, and height. Together, these factors affect the magnitude and ratio of radiation, sensible, and latent heat fluxes and, therefore, must be considered during field recordings [50]. The highest ΔT values were recorded shortly before and after noon, when the global radiation and thus the absorption of radiative heat were highest. Under these conditions, the effect of evaporative cooling was highest as high transpiration rates are driven by radiation and the leaf-to-air vapor pressure deficit. Monitoring GI on warm and sunny days should therefore produce the clearest signals of drought stress. This is in accordance with Grant et al. [51] and confirmed to be the best time to detect water-stress-induced temperature differences. For practical applications, however, it will be necessary to determine absolute temperatures using a blackbody for calibration because neither stressed nor non-stressed plants can be differentiated as a reference to calculate ΔT in the field.

As shown in Figure 5, all four species closed their stomata with the onset of drought stress, expressed by the decrease of stomatal conductance. The effects were species specific, as *Geranium* and *Heuchera* showed symptoms of stress earlier than *Brunnera* and *Bergenia*. The leaf surface warmed due to the lack of water molecules vaporizing in the leaf intercellulars and transpired to the atmosphere via the stomata, which is consistent with the work of Katul et al. [52]. The latent heat exchange through transpiration from the water-stressed plants could not be maintained because no water vapor diffused through the stomata and therefore leaf temperature increased [53]. Considering the leaf energy balance, stressed leaves heat up because they cannot compensate for the radiative energy transfer by the latent heat flux [27]. Thereby, they warm and balance radiative heat input by convective loss (when leaves are warmer than ambient air), which heats the surrounding air [54]. Without radiation input after sunset, the temperatures of the stressed and the control group were almost identical again. In the control group, however, the leaf was cooled by latent heat loss below the air temperature, which, in exchange, results in sensible heat flux from the air to the leaf to keep the leaf energy balance in equilibrium [40,55,56]. The leaf temperature varies between species due to physical and physiological differences, e.g., leaf hairs that reflect radiation or increase the boundary layer resistance, smaller leaves with increased heat convection, or succulent leaves that have low transpiration [57–59]. Lin et al. [60] proved that transpiration is a more effective way to cool leaves than physical traits such as leaf hairs or smaller leaves when water is sufficient. Plants that maximize transpiration rates to tolerate high temperatures through heat loss have high stomatal conductance, either due to large stomata or a large number of stomata [61]. This strategy requires a sufficient water supply, but if given, the cooling effect of transpiration can be increased by plant selection, considering parameters such as the leaf area index, vertical canopy thickness, and total vegetation coverage [16,22].

This is specifically important when it comes to planning and managing GIs for UHI mitigation and urban microclimatic regulation. In technically and highly advanced systems such as LWSs and systems sensitive to dehydration, automated and sensor-based irrigation are about to be established as state-of-the-art [18,62]. Smart irrigation allows for demand-based water supply. However, this raises the cost of already high-priced technologies and maintenance efforts. Simple and low-budget solutions such as soil-based and pot-based systems usually do not require permanent irrigation. Balancing water storage capacities and plant availability of technical substrates is therefore decisive.

Whenever weather conditions might cause long-lasting droughts and raise the risk of stress-induced shortfalls or losses, TIRs are a promising tool to support the monitoring of water stress in GI. The implementation and enhancement of GI for urban microclimate regulation and climate change adaptation are important measures that require strategic planning and management [7]. This will only succeed when the efficiency and benefits of

GI and their physiological functions are secured and accordingly controlled. TIR offers a promising tool to assist in monitoring water stress in GI and can be used to quantify the species-specific cooling potential. Further research using continuous thermal records could provide insights into the cooling potential of different GIs, which is affected by the relationship between leaf surface temperature and stomatal conductance of different species. Securing and controlling the physiological functions and requirements will enhance the efficiency, functionality, and sustainability of GIs.

The data presented give first and novel insights into the magnitude of temperature differences between well-watered and stressed façade greenery plants and thus their potential cooling effect.

5. Conclusions

Based on our findings and the comprehensive literature, we conclude that for urban green infrastructure (GI) to fulfill appropriate cooling functions, the plants used must be adequately supplied with water. These findings contribute to the understanding of the quantification of the cooling effects of plants in GIs and provide a basis for further research. The method used to quantify temporal temperature developments is promising for further investigations to advance detailed monitoring and exploration of urban GI in terms of urban ecosystems and the services they rely on. Especially the use of UAVs could complement ground-based manual inspections and therefore may be useful tools for monitoring the status of GI in cities. To detect drought stress, we recommend monitoring on sunny days around noon when solar radiation is highest and when the effect of drought stress is seen most clearly.

Author Contributions: Conceptualization, M.G., M.I., and R.S.; methodology, M.G. and M.I.; investigation, M.G. and M.I.; resources, M.I., R.S., and P.H.; data curation, M.G. and M.I.; writing—original draft preparation, M.G.; writing—review and editing, M.G., R.S., M.I., and P.H.; visualization, M.G.; supervision, M.I. and R.S.; project administration, M.I. and R.S.; funding acquisition, R.S. and M.I. All authors have read and agreed to the published version of the manuscript.

Funding: This research was funded by Austrian Research Promotion Agency (FFG)-technology program “City of Tomorrow”, Grant Number 867366. Open access funding provided by BOKU Vienna Open Access Publishing Fund.

Institutional Review Board Statement: Not applicable.

Informed Consent Statement: Not applicable.

Data Availability Statement: The data presented in this study are available on request from the corresponding authors.

Acknowledgments: Many thanks to Gerhard Wagner for making the glass house available, to Max Kampen and Stefan Lederbauer for the support with the measurements, Bernhard Spangl for statistical support, Pia Minixhofer and Bernhard Kastner for proofreading.

Conflicts of Interest: The authors declare no conflict of interest. The funders had no role in the design of the study; in the collection, analyses, or interpretation of data; in the writing of the manuscript, or in the decision to publish the results.

References

1. Lee, T.-W.; Lee, J.Y.; Wang, Z.-H. Scaling of the urban heat island intensity using time-dependent energy balance. *Urban Clim.* **2012**, *2*, 16–24. [[CrossRef](#)]
2. Aram, F.; Higuera García, E.; Solgi, E.; Mansournia, S. Urban green space cooling effect in cities. *Heliyon* **2019**, *5*, e01339. [[CrossRef](#)]
3. Santamouris, M. On the energy impact of urban heat island and global warming on buildings. *Energy Build.* **2014**, *82*, 100–113. [[CrossRef](#)]
4. Paravantis, J.; Santamouris, M.; Cartalis, C.; Efthymiou, C.; Kontoulis, N. Mortality Associated with High Ambient Temperatures, Heatwaves, and the Urban Heat Island in Athens, Greece. *Sustainability* **2017**, *9*, 606. [[CrossRef](#)]
5. Zinzi, M.; Santamouris, M. Introducing Urban Overheating—Progress on Mitigation Science and Engineering Applications. *Climate* **2019**, *7*, 15. [[CrossRef](#)]

6. Oke, T.R. The energetic basis of the urban heat island. *Q. J. R. Meteorol. Soc.* **1982**, *108*, 1–24. [[CrossRef](#)]
7. Bowler, D.E.; Buyung-Ali, L.; Knight, T.M.; Pullin, A.S. Urban greening to cool towns and cities: A systematic review of the empirical evidence. *Landsc. Urban Plan.* **2010**, *97*, 147–155. [[CrossRef](#)]
8. Leal Filho, W.; Echevarria Icaza, L.; Neht, A.; Klavins, M.; Morgan, E.A. Coping with the impacts of urban heat islands. A literature based study on understanding urban heat vulnerability and the need for resilience in cities in a global climate change context. *J. Clean. Prod.* **2018**, *171*, 1140–1149. [[CrossRef](#)]
9. Semeraro, T.; Scarano, A.; Buccolieri, R.; Santino, A.; Aarrevaara, E. Planning of Urban Green Spaces: An Ecological Perspective on Human Benefits. *Land* **2021**, *10*, 105. [[CrossRef](#)]
10. Minixhofer, P.; Stangl, R. Green Infrastructures and the Consideration of Their Soil-Related Ecosystem Services in Urban Areas—A Systematic Literature Review. *Sustainability* **2021**, *13*, 3322. [[CrossRef](#)]
11. Akbari, H.; Cartalis, C.; Kolokotsa, D.; Muscio, A.; Pisello, A.L.; Rossi, F.; Santamouris, M.; Synnef, A.; Wong, N.H.; Zinzi, M. Local climate change and urban heat island mitigation techniques—The state of the art. *J. Civ. Eng. Manag.* **2015**, *22*, 1–16. [[CrossRef](#)]
12. Kabisch, N.; Korn, H.; Stadler, J.; Bonn, A. Nature-Based Solutions to Climate Change Adaptation in Urban Areas—Linkages Between Science, Policy and Practice. In *Nature-Based Solutions to Climate Change Adaptation in Urban Areas*; Kabisch, N., Korn, H., Stadler, J., Bonn, A., Eds.; Springer International Publishing: Cham, Switzerland, 2017; pp. 1–11. ISBN 978-3-319-53750-4.
13. European Environment Agency. *Green Infrastructure and Territorial Cohesion: The Concept of Green Infrastructure and Its Integration into Policies Using Monitoring Systems (EEA Technical Report No 18/2011)*; EEA Technical Report No 18; European Environment Agency: København, Denmark, 2011. [[CrossRef](#)]
14. Hunter, A.B.; Livesley, J.S.; Williams, S.G.N. Responding to the Urban Heat Island: A Review of the Potential of Green Infrastructures: Report Funded by the Victorian Centre for Climate Change Adaptation (VCCCAR). Melbourne, Australia. 2012. Available online: <https://apo.org.au/sites/default/files/resource-files/2012-03/apo-nid237206.pdf> (accessed on 31 March 2021).
15. Wilby, R.L. A Review of Climate Change Impacts on the Built Environment. *Built Environ.* **2007**, *31*, 31–45. [[CrossRef](#)]
16. Wootton-Beard, P.; Xing, Y.; Durai Prabhakaran, R.; Robson, P.; Bosch, M.; Thornton, J.; Ormondroyd, G.; Jones, P.; Donnison, I. Review: Improving the Impact of Plant Science on Urban Planning and Design. *Buildings* **2016**, *6*, 48. [[CrossRef](#)]
17. Coutts, A.M.; Daly, E.; Beringer, J.; Tapper, N.J. Assessing practical measures to reduce urban heat: Green and cool roofs. *Build. Environ.* **2013**, *70*, 266–276. [[CrossRef](#)]
18. Medl, A.; Stangl, R.; Florineth, F. Vertical greening systems—A review on recent technologies and research advancement. *Build. Environ.* **2017**, *125*, 227–239. [[CrossRef](#)]
19. Kromoser, B.; Ritt, M.; Spitzer, A.; Stangl, R.; Idam, F. Design Concept for a Greened Timber Truss Bridge in City Area. *Sustainability* **2020**, *12*, 3218. [[CrossRef](#)]
20. Taleghani, M. Outdoor thermal comfort by different heat mitigation strategies—A review. *Renew. Sustain. Energy Rev.* **2018**, *81*, 2011–2018. [[CrossRef](#)]
21. Bartesaghi Koc, C.; Osmond, P.; Peters, A. Evaluating the cooling effects of green infrastructure: A systematic review of methods, indicators and data sources. *Solar Energy* **2018**, *166*, 486–508. [[CrossRef](#)]
22. Skelhorn, C.; Lindley, S.; Levermore, G. The impact of vegetation types on air and surface temperatures in a temperate city: A fine scale assessment in Manchester, UK. *Landsc. Urban Plan.* **2014**, *121*, 129–140. [[CrossRef](#)]
23. Cameron, R.W.F.; Taylor, J.E.; Emmett, M.R. What’s ‘cool’ in the world of green façades? How plant choice influences the cooling properties of green walls. *Build. Environ.* **2014**, *73*, 198–207. [[CrossRef](#)]
24. Zupancic, T.; Westmacott, C.; Bulthuis, M. *The Impact of Green Space on Heat and Air Pollution in Urban Communities: A Meta-Narrative Systematic Review*; David Suzuki Foundation: Vancouver, BC, Canada, 2015.
25. Vidrih, B.; Medved, S. Multiparametric model of urban park cooling island. *Urban For. Urban Green.* **2013**, *12*, 220–229. [[CrossRef](#)]
26. Zardo, L.; Geneletti, D.; Pérez-Soba, M.; van Eupen, M. Estimating the cooling capacity of green infrastructures to support urban planning. *Ecosyst. Serv.* **2017**, *26*, 225–235. [[CrossRef](#)]
27. Nobel, P.S. *Physicochemical and Environmental Plant Physiology*; Academic Press: Cambridge, MA, USA, 1991.
28. Ihuoma, S.O.; Madramootoo, C.A. Recent advances in crop water stress detection. *Comput. Electron. Agric.* **2017**, *141*, 267–275. [[CrossRef](#)]
29. Rahman, M.A.; Moser, A.; Rötzer, T.; Pauleit, S. Within canopy temperature differences and cooling ability of *Tilia cordata* trees grown in urban conditions. *Build. Environ.* **2017**, *114*, 118–128. [[CrossRef](#)]
30. Buckley, T.N. How do stomata respond to water status? *New Phytol.* **2019**, *224*, 21–36. [[CrossRef](#)] [[PubMed](#)]
31. Jones, H.G. Irrigation scheduling: Advantages and pitfalls of plant-based methods. *J. Exp. Bot.* **2004**, *55*, 2427–2436. [[CrossRef](#)] [[PubMed](#)]
32. Jones, H.G. Use of thermography for quantitative studies of spatial and temporal variation of stomatal conductance over leaf surfaces. *Plant Cell Environ.* **1999**, *22*, 1043–1055. [[CrossRef](#)]
33. Parkash, V.; Singh, S. A Review on Potential Plant-Based Water Stress Indicators for Vegetable Crops. *Sustainability* **2020**, *12*, 3945. [[CrossRef](#)]
34. Taghvaeian, S.; Comas, L.; DeJonge, K.C.; Trout, T.J. Conventional and simplified canopy temperature indices predict water stress in sunflower. *Agric. Water Manag.* **2014**, *144*, 69–80. [[CrossRef](#)]

35. Gardner, B.R.; Blad, B.L.; Garrity, D.P.; Watts, D.G. Relationships between crop temperature, grain yield, evapotranspiration and phenological development in two hybrids of moisture stressed sorghum. *Irrig. Sci.* **1981**, *213–224*. [[CrossRef](#)]
36. DeJonge, K.C.; Taghvaeian, S.; Trout, T.J.; Comas, L.H. Comparison of canopy temperature-based water stress indices for maize. *Agric. Water Manag.* **2015**, *156*, 51–62. [[CrossRef](#)]
37. Smigaj, M.; Gaulton, R.; Suarez, J.; Barr, S. Use of Miniature Thermal Cameras for Detection of Physiological Stress in Conifers. *Remote Sens.* **2017**, *9*, 957. [[CrossRef](#)]
38. Kelly, J.; Kljun, N.; Olsson, P.-O.; Mihai, L.; Liljeblad, B.; Weslien, P.; Klemedtsson, L.; Eklundh, L. Challenges and Best Practices for Deriving Temperature Data from an Uncalibrated UAV Thermal Infrared Camera. *Remote Sens.* **2019**, *11*, 567. [[CrossRef](#)]
39. Georgi, N.J.; Zafiriadis, K. The impact of park trees on microclimate in urban areas. *Urban Ecosyst.* **2006**, *9*, 195–209. [[CrossRef](#)]
40. Gupta, S.K.; Ram, J.; Singh, H. Comparative Study of Transpiration in Cooling Effect of Tree Species in the Atmosphere. *GEP* **2018**, *6*, 151–166. [[CrossRef](#)]
41. Senior, R.A.; Hill, J.K.; Edwards, D.P. ThermStats: An R package for quantifying surface thermal heterogeneity in assessments of microclimates. *Methods Ecol. Evol.* **2019**, *10*, 1606–1614. [[CrossRef](#)]
42. Eilers, P.H.C. A perfect smoother. *Anal. Chem.* **2003**, *75*, 3631–3636. [[CrossRef](#)] [[PubMed](#)]
43. Atzberger, C.; Eilers, P.H.C. Evaluating the effectiveness of smoothing algorithms in the absence of ground reference measurements. *Int. J. Remote Sens.* **2011**, *32*, 3689–3709. [[CrossRef](#)]
44. Sagan, V.; Maimaitijiang, M.; Sidike, P.; Eblimit, K.; Peterson, K.; Hartling, S.; Esposito, F.; Khanal, K.; Newcomb, M.; Pauli, D.; et al. UAV-Based High Resolution Thermal Imaging for Vegetation Monitoring, and Plant Phenotyping Using ICI 8640 P, FLIR Vue Pro R 640, and thermoMap Cameras. *Remote Sens.* **2019**, *11*, 330. [[CrossRef](#)]
45. Kassambara, A. Rstatix: Pipe-Friendly Framework for Basic Statistical Tests. R Package Version 0.6.0. 2020. Available online: <https://cran.r-project.org/web/packages/rstatix/index.html> (accessed on 31 March 2021).
46. Grant, O.M.; Tronina, L.; Jones, H.G.; Chaves, M.M. Exploring thermal imaging variables for the detection of stress responses in grapevine under different irrigation regimes. *J. Exp. Bot.* **2007**, *58*, 815–825. [[CrossRef](#)]
47. Sheng, H.; Chao, H.; Coopman, C.; Han, J.; Mckee, M.; Chem, Y. Low-Cost UAV-Based Thermal Infrared Remote Sensing Platform, Calibration and Applications. In Proceedings of the International Conference on Mechatronic and Embedded Systems and Applications, Qingdao, China, 15–17 July 2010; pp. 38–43. [[CrossRef](#)]
48. Tanner, C.B. Plant Temperatures. *Agron. J.* **1963**, *55*, 201–211. [[CrossRef](#)]
49. Costa, J.M.; Grant, O.M.; Chaves, M.M. Thermography to explore plant-environment interactions. *J. Exp. Bot.* **2013**, *64*, 3937–3949. [[CrossRef](#)] [[PubMed](#)]
50. Maes, W.H.; Steppe, K. Estimating evapotranspiration and drought stress In *Posidonia oceanica* cadmium induces changes with ground-based thermal remote sensing in methylation and chromatin patterning agriculture: A review. *J. Exp. Bot.* **2012**, *63*, 695–709. [[CrossRef](#)] [[PubMed](#)]
51. Grant, O.M.; Chaves, M.M.; Jones, H.G. Optimizing thermal imaging as a technique for detecting stomatal closure induced by drought stress under greenhouse conditions. *Physiol. Plant.* **2006**, *127*, 507–518. [[CrossRef](#)]
52. Katul, G.G.; Oren, R.; Manzoni, S.; Higgins, C.; Parlange, M.B. Evapotranspiration: A process driving mass transport and energy exchange in the soil-plant-atmosphere-climate system. *Rev. Geophys.* **2012**, *50*, 1083. [[CrossRef](#)]
53. Barthakur, N. Leaf temperatures under controlled environmental conditions. *Int. J. Biometeorol.* **1975**, *19*, 21–27. [[CrossRef](#)]
54. Gutschick, V.P. Leaf Energy Balance: Basics, and Modeling from Leaves to Canopies. In *Canopy Photosynthesis: From Basics to Applications*; Hikosaka, K., Niinemets, Ü., Anten, N.P.R., Eds.; Springer: Dordrecht, The Netherlands, 2016; pp. 23–58. ISBN 978-94-017-7290-7.
55. Gates, D.M. *Biophysical Ecology*; Springer: New York, NY, USA, 1980. [[CrossRef](#)]
56. Yu, M.-H.; Ding, G.-D.; Gao, G.-L.; Sun, B.-P.; Zhao, Y.-Y.; Wan, L.; Wang, D.-Y.; Gui, Z.-Y. How the Plant Temperature Links to the Air Temperature in the Desert Plant *Artemisia ordosica*. *PLoS ONE* **2015**, *10*, e0135452. [[CrossRef](#)]
57. Martin, T.A.; Hinckley, T.M.; Meinzer, F.C.; Sprugel, D.G. Boundary layer conductance, leaf temperature and transpiration. *Tree Physiol.* **1998**, 435–443. [[CrossRef](#)]
58. Ye, C.; Li, M.; Hu, J.; Cheng, Q.; Jiang, L.; Song, Y. Highly reflective superhydrophobic white coating inspired by poplar leaf hairs toward an effective “cool roof”. *Energy Environ. Sci.* **2011**, *4*, 3364. [[CrossRef](#)]
59. Yates, M.J.; Anthony Verboom, G.; Rebelo, A.G.; Cramer, M.D. Ecophysiological significance of leaf size variation in Proteaceae from the Cape Floristic Region. *Funct. Ecol.* **2010**, *24*, 485–492. [[CrossRef](#)]
60. Lin, H.; Chen, Y.; Zhang, H.; Fu, P.; Fan, Z. Stronger cooling effects of transpiration and leaf physical traits of plants from a hot dry habitat than from a hot wet habitat. *Funct. Ecol.* **2017**, *31*, 2202–2211. [[CrossRef](#)]
61. Jones, H.G.; Rotenberg, E. *Energy, Radiation and Temperature Regulation in Plants*; John Wiley & Sons, Ltd.: Chichester, UK, 2001; p. 90. ISBN 0470016175.
62. Radić, M.; Brković Dodig, M.; Auer, T. Green Facades and Living Walls—A Review Establishing the Classification of Construction Types and Mapping the Benefits. *Sustainability* **2019**, *11*, 4579. [[CrossRef](#)]